The loci of oscillatory visual-object priming: a combined electroencephalographic and reaction-time study

ELSEVIER

International Journal of Psychophysiology 38 (2000) 225–241

INTERNATIONAL JOURNAL OF PSYCHOPHYSIOLOGY

www.elsevier.nl/locate/ijpsycho

The loci of oscillatory visual-object priming: a combined electroencephalographic and reaction-time study

Mark A. Elliott[a,*], Christoph S. Herrmann[b], Axel Mecklinger[b], Hermann J. Müller[a]

[a] *Institut Für Allgemeine Psychologie, Universität Leipzig, Leipzig, Germany*
[b] *Max-Planck Institute of Cognitive Neuroscience, Leipzig, Germany*

Received 28 September 1999; accepted 15 May 2000

Abstract

The detection of reaction-times (RTs) to a target Kanizsa-type square (an illusory square defined by the collinear arrangement of 90° corner junctions) within a matrix of distractor junctions are expedited when the target display is preceded by a 40-Hz flickering display of premask crosses presented prior to, and at the locations subsequently occupied by the junctions of the target display. Priming effects were obtained when four crosses (which together matched the Gestalt arrangement of the target) were presented at the display locations subsequently occupied by the junctions forming the target Kanizsa square (Elliott and Müller, 1998; Elliott and Müller, 2000). The present study was conducted with the aim of replicating the 40-Hz RT priming effects, while simultaneously recording the observers EEG in order to establish the presence and location of Gestalt priming in the brain. The statistical pattern obtained in the RT data corresponded well with previous studies and was matched by the pattern of target P300 latencies across bilateral central and posterior electrodes. Planned analyses focused upon the evoked 40-Hz activity that co-occurs with the P300, revealing a more specific pattern of 40-Hz priming over the visual cortex. A subsequent series of cross-correlational analyses examined the cortical distribution and timing of Gestalt-prime generation during and subsequent to premask-display presentation. Correlations were revealed between stimulus related 40-Hz activity over a range of cortical loci, including the right temporal lobe, which is considered important for figure coding. Taken together, these findings not only support the role of a distributed 40-Hz mechanism during Gestalt-figure priming, but also suggest that patterns of oscillatory brain activity may be directly influenced by, and interpretable in terms of equivalent temporal patterns of stimulus activity.

Keywords: Visual-Gestalt priming; Object coding; Kanizsa-type figure detection; Reaction time; EEG; Wavelet transform; Evoked gamma-band activity

* Corresponding author. Tel.: +49-341-973-5957; fax: +49-341-973-5969.
E-mail address: elliott@uni-leipzig.de (M.A. Elliott).

0167-8760/00/$ - see front matter
PII: S0167-8760(00)00167-7

1. Introduction

In order to successfully combine the separable feature-elements of a visual object into a single perceptual item, the feature-elements must be first differentiated and then recombined or 'bound' into a composite 'object' representation. Composite featural representations have been shown to be represented in the 'ventral' visual pathways (Ungerleider and Mishkin, 1982) which includes the temporal cortex and, particularly, the inferotemporal cortex (IT, see Desimone et al., 1984; Fujita et al., 1992; Moran and Desimone, 1985). In addition, motion-coding areas in the 'dorsal' visual pathways, such as the medial-temporal cortex (MT), are capable of responding to the motion of Gestalt configurations within their receptive fields (Logothesis and Schall, 1989). Neurophysiological studies have demonstrated that basic feature-elements are coded earlier than in either IT or MT, by anatomically and functionally specific visuo-cortical neurons tuned to particular physical attributes of the stimulus (e.g. Hubel and Wiesel, 1959; Livingstone and Hubel, 1988). It has also been demonstrated that feature-coding neurons in the visual cortex adjust their firing pattern and fire synchrony if separate stimulus features belong to the same object. These findings suggest that the 'binding' of feature-elements is achieved through temporal coordination of local activity in the visual cortex (e.g. Gray et al., 1989; Kreiter and Singer, 1992; Eckhorn et al., 1993; Frien et al., 1994), which supports the Gestalt grouping of stimulus elements according to criteria such as stimulus continuity, the proximity and common motion of stimuli (Engel et al., 1991; Gray et al., 1989).

Electroencephalographic (EEG) recordings have also shown that gamma-band activity specific to posterior electrodes varies with common stimulus motion (Lutzenberger et al., 1995; Müller et al., 1996, 1997) and is selectively enhanced when observers are asked to silently count targets that group according to continuity (Herrmann et al., 1999; Tallon et al., 1995). In addition, these and other EEG studies have also reported stimulus-specific gamma-band activity across a wider area of cortex: Başar-Eroglu et al. (1996a), Herrmann et al., (1999), Tallon-Baudry et al. (1996, 1997) have reported gamma-band activity across frontal, central and temporal electrodes as well as posterior electrodes during visuo-perceptual tasks, including the perception of multistable stimuli, visual classification and search for a target embedded amongst distractor items (respectively). The distribution of gamma-band activity across a range of brain areas corresponds well with the idea that performance on visuo-perceptual tasks such as visual grouping and object selection is mediated by mechanisms outside of the visual cortex, which has also encouraged speculation that the synchronization of neuronal firing at earlier stages of visual coding is influenced in a top-down fashion by activity at later stages (see Başar-Eroglu et al., 1996b; Singer, 1996).

In agreement with this idea, recent behavioral evidence has shown that an undetected, but figurally-relevant, priming stimulus may segment from a fully visible display of flickering premask crosses and thereby prime the reaction time (RT) response to a target-figure, subsequently presented at the same matrix location as the figural prime (i.e. the priming effect was spatially specific, see Elliott and Müller, 1998, Experiment 3). Priming was also both target- and frequency-specific and occurred only if the flicker frequency across the premask display was set at 40 Hz and not at the other mid-gamma-band frequencies tested (note that the premask display consisted of four temporally and spatially separate image frames that repeated at 10 Hz; image frames were presented sequentially, each frame for 25 ms with a 0-ms interval between frames). For a 40-Hz flicker, observers were unable to detect the spatio-temporal structure of the premask display, although the prime persisted as a form of short-term visual memory for 240–300 ms, a duration consistent with that of a 'visible' stimulus (Coltheart, 1980; Elliott and Müller, 2000). Furthermore, across the duration of prime persistence, the RTs to the target figure displayed a clear 40-Hz periodicity that was confined to trials upon which a figurally-relevant priming stimulus was presented. These findings confirmed that the internal response to prime display presentation was a process that matched the 40-Hz structure of the premask

display, which was specific to the figural coding mechanisms responsible for prime generation.

The figure-ground segmentation account for frequency-specific priming logically entails that the prime must be coded in the context of the premask display as a whole. The evidence outlined above supports this idea and also advances the idea that the prime becomes active across a number of contributive visual-coding mechanisms. Consider the finding that prime persistence is consistent with that of a visible stimulus, although the priming stimulus is not itself detected. In addition, the priming effects are spatially specific, suggesting that the prime becomes active at an early stage of visual coding where neurons respond to activity across relatively small regions of visual space (the products of which are not consciously available, see He et al., 1996), but inherits (persistence) properties consistent with the later coding of a visible stimulus; in this instance the premask display as a whole. One candidate location for the coding of the premask display has been suggested as IT (Elliott and Müller, 2000). Taken together, the accumulated evidence and speculations concerning the priming effect suggest that the prime develops an oscillatory structure across early visual-coding mechanisms through the backpropagation of an oscillatory code, which is generated across later mechanisms such as IT, and which would permit the prime to develop a periodic structure consistent with the 40-Hz periodicity of the premask-display as a whole.

In the current investigation, the RT paradigm described by Elliott and Müller (1998) was combined with EEG recording in order to examine a series of hypotheses related to the locus of the 40-Hz prime activity. Given that the previous evidence for 40-Hz oscillatory priming was based upon RT measures, as a first step, it was proposed to examine for prominent event-related potentials (ERPs) that showed evidence of prime activity matching the pattern of effects revealed within the accompanying RT data. The RTs were specifically expected to reveal target-specific priming (demonstrated by a significant interaction of target and prime) with no influence of priming on target-absent trials. Thus, for ERPs following target presentation, an equivalent pattern of effects would be considered characteristic of prime activity, although for ERPs revealed during premask display presentation (i.e. prior to presentation of the target display), this criterion was relaxed to include any significant evidence of prime activity, irrespective to the subsequent presentation of a target on those trials.

As mentioned above, the RT data of Elliott and Müller (2000) have also shown that the internal response to prime-display presentation was a figural-coding process with a 40-Hz structure. Accordingly, it was proposed to specifically examine the 40-Hz EEG response at those electrodes for which a target $\times$ prime interactions were examined in the ERP. There is evidence that the neural response to flickering stimulation matches the frequency of the stimulus (Gur and Snodderly, 1997), and a temporal correspondence between ERP components, such as the N1 or the P300, with stimulus-related 40-Hz activity has been suggested by previous studies (Başar et al., 1993; Herrmann et al., 1999). These findings influenced the choice of the wavelet analysis used in this study, which was primarily based upon the following considerations: Elliott and Müller (1998), Elliott and Müller (2000) have shown that the response to a 40-Hz flickering display which contains a figurally-relevant priming stimulus is the formation of a spatially-specific prime with a 40-Hz structure, which is phase-locked to the presentation sequence of the premask frames. This translation of the global 40-Hz rhythm to the local response to the priming stimulus might only be achieved if the 40-Hz neural response is backpropagated from visual coding areas such as IT, which code across the entire premask display, to mechanisms (in the visual cortex, for example), which code local subregions of the display. The idea that object representations are generated through recurrent activity in the brain is consistent with the findings of some recent EEG studies (see Tallon-Baudry and Bertrand, 1999), although the idea that the pattern of prime activity is 'evoked' by stimulus presentation is inconsistent with the findings of these researchers, who state that figure coding processes occur in the 'induced' (i.e. non-phase locked) gamma-band response to

stimulus presentation. However, other investigations of the gamma band response to figure presentation have shown the opposite pattern of effects (see, Herrmann et al., 1999). Herrmann et al. showed that a stimulus-specific response to illusory Kanizsa figures (also employed by Tallon et al., 1995) were precisely time locked to stimulus presentation. Given the consistency of the 'evoked' gamma-band account with the priming effects shown by Elliott and Müller (2000), it was proposed to focus upon the 40-Hz response, which was time locked to premask display presentation, for evidence of prime operation.

It was considered logical that those electrodes at which the 40-Hz EEG revealed differences between figurally relevant and non-relevant premasks, equivalent or similar to those found in the RTs, could be considered indicators of prime activity and, therefore, candidate loci for prime generation and persistence. Given that the priming effects may be principally determined by the 10-Hz EEG response to the repeat of the individual premask-frames, which should also be strongly represented in the evoked EEG response, additional (and identical) analyses examined the 10-Hz EEG response that co-occurred with the ERP. The separate analyses of 10- and 40-Hz EEG responses were considered legitimate on the basis of the proposal (see Başar-Eroglu and Başar, 1991) that the 10- and 40-Hz EEG should be considered in terms of qualitatively different types of stimulus-processing mechanisms. For the ERP, the 10- and 40-Hz EEG analyses, the likely loci of prime activity were expected to be indicated by the electrodes at which target-specific differences in prime amplitudes (i.e. target $\times$ prime interactions) were reliably obtained (i.e. given target $\times$ prime $\times$ electrode interactions).

Having identified the most likely loci for prime activity, a subsequent cross-correlational analysis was planned to examine the related hypothesis that the prime activity was not confined to single, independent mechanisms, but was generated across a series of visual coding areas. It was expected that the crosscorrelational analysis would reveal a relationship between loci at which (i) the synchronous prime might become 'locally' active at 40 Hz with (ii) loci at which the coding of global properties of the premask display might encourage the generation of the 40-Hz code adopted by the prime. Finally, the cross-correlational design was considered suitable across a series of time windows from the trial onset to target response in order to capture patterns of activity during time periods prior to the onset of the target stimulus (recall that the priming EEG effect can only occur in the time period during, or immediately after premask-display presentation).

2. Method

2.1. Observers

Eleven observers participated in the experiment (eight male; mean age 24.3 years; all with normal or corrected-to-normal vision).

2.2. Design and procedure

The experiment used a within-subject design, with stimulus parameters similar to those used previously (see Elliott and Müller, 1998). A trial always started with a brief (300-ms) 250-Hz computer-generated tone. Following a subsequent delay of 200 ms, observers were presented with the flickering 3×3 matrix of premask crosses, which after 600 ms, reduced to simple 90° corner junctions by the removal of redundant line segments (see Fig. 1a). Observers were informed that the flickering display did not require a response, but that they should fixate to the center of the display and avoid eye-movements during presentation. On removal of the redundant line segments, observers were asked to produce an RT response, as rapidly and accurately as possible, to the presence or absence of a target Kanizsa-type square within the matrix of 90° corner junctions (see Fig. 1a). In the event of an erroneous response, feedback was provided through a second (150-ms) 100-Hz computer-generated tone followed by a 500-ms delay.

The premask crosses comprised four separate frames, the members of which were presented simultaneously, but asynchronously relative to the

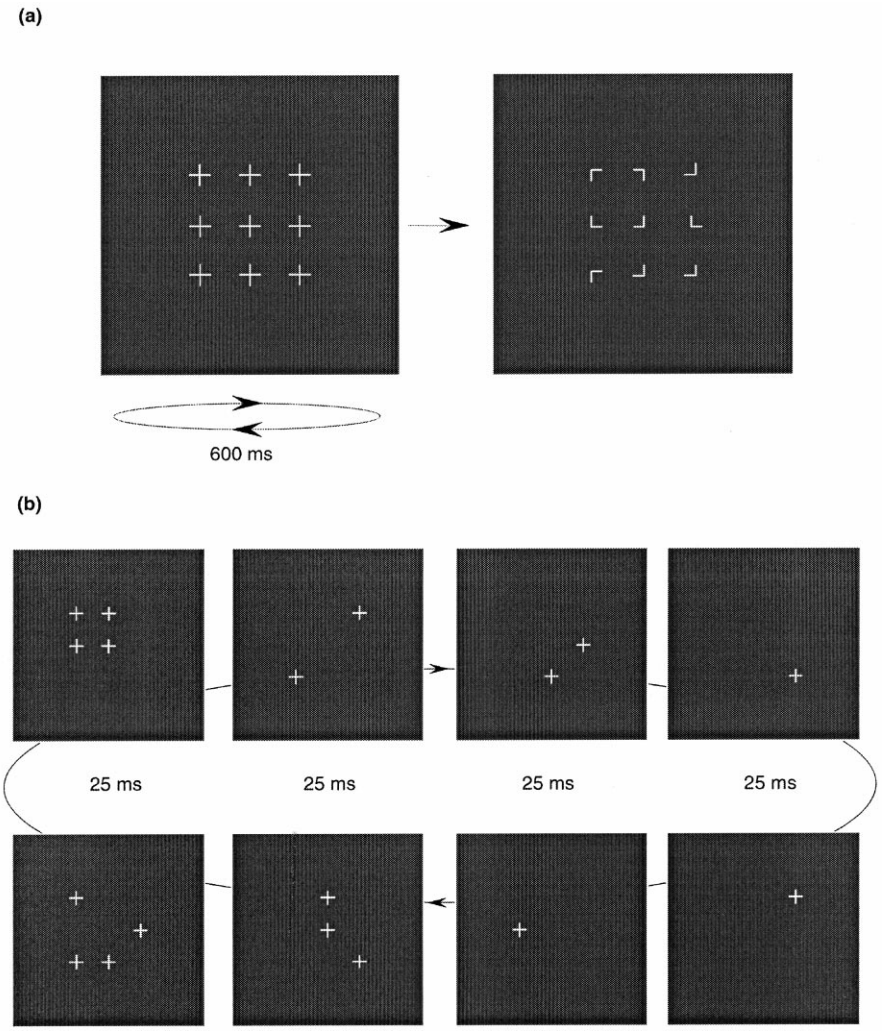

Fig. 1. The stimulus presentation paradigm. In (a), the premask-display presentation was followed by a target display to which the observers produced their target-present/absent RT responses. In (b) are shown example sequences of the four premask frames in both no-prime and prime condition, which includes a premask consisting of four elements presented in square arrangement (upper left panel).

members of other frames. As illustrated in Fig. 1b, this design permitted two premask conditions to be defined, the 'prime' and 'no-prime' conditions. In the prime condition, one subset of premask elements consisted of four crosses presented at the display locations subsequently occupied by corner junctions defining the target Kanizsa-type square. In the no-prime condition, there was also one subset comprising four elements, which were, however, presented in pseudo-random arrangement that did not correspond to a square. Pre-mask displays were presented for 600 ms and the presentation frequency across the entire premask display was maintained at 40 Hz. Thus, at 40 Hz, the entire premask matrix (i.e. the sequence of all four premask frames) was presented 10 times per 1000 ms (i.e. each premask frame repeated at 10 Hz), with a constant frame exposure duration of 25 ms and an inter-subset interval of less than 1 ms. In this

way, the premask sequence was continually 'recycled' during the lead time to target display onset. This produced the phenomenal experience of a flickering display of nine crosses, within which observers were unable to discern the structure of a given frame. Target and non-target displays did not oscillate, but were presented until a response keypress.

All conditions were presented in pseudo-random order within each of eight, 40-trial blocks and were preceded by one block of randomized practice trials immediately prior to the experiment proper. The observers were naive to the precise experimental conditions presented in each experiment and received payment at the rate of DM 15.00 per hour.

2.3. Apparatus and stimuli

Stimulus event timing and EEG trigger signals, data collection and image frame generation were controlled by a PC-compatible computer which also controlled oscilloscopic image presentation through an Interactive Electronics Systems point plotter buffer with a 8-Mb frame store memory (Finley, 1985). Image frames were presented on a 6″ Tektronix 608-oscilloscope monitor equipped with a very fast-decay P15 phosphor. The use of a P15 phosphor ensured that on-screen image persistence reduced to 10% of normal image intensity within 2.8 μs of image termination (Bell, 1970). The Interactive Electronic Systems point plotter buffer allowed pixels to be plotted at a rate of one pixel every microsecond. Although individual premask-image frames were repeatedly presented at 10 Hz, both oscillatory and static (target-display) frames were displayed at a background presentation frequency of 1 kHz.

In order to encourage EEG activity of sufficient amplitude to permit successful time-frequency analysis, both the size and brightness of the premask and target stimuli were increased in comparison with the stimulus dimensions previously employed. Stimulus luminance was increased to 1.2 cd/m^2 upon a background field of 0.075 cd/m^2 with a mean screen-surround luminance of 0.078 cd/m^2. Observers viewed the oscilloscope monitor at a distance of 38 cm (maintained via a chin rest), thereby increasing the retinal size of display elements by 150% relative to the size of similar 3×3 element displays to those used in previous experiments. Finally, both premask and target specified-to-total inducer length parameters were increased from 20% to 40%. The reliability of the 40% inducer length parameter for production of the RT priming effect was established by a pilot experiment.

Pre-mask crosses subtended 2°33′ of the visual angle, and exhibited horizontal and vertical separations of 2°42′. This produced premask displays in which the 3×3 matrix of premask elements subtended either 13°03′ × 13°03′ of the visual angle (frame elements were arranged around the center of the monitor screen). Pre-mask crosses comprised 21 pixels and along each axis of the premask cross, pixels were separated by 16′03″ of visual angle. No gap was visible between each pixel and stimuli appeared as conjunctions of uninterrupted lines. Pre-mask frames could consist of one, two, three or four elements presented simultaneously; thus the amount of pixels presented in a given frame could be either 21, 42, 63 or 84. This could result in the brightness of premask stimuli varying across frames, with frames comprising fewer elements appearing brighter than those with more elements. In order to control for differential stimulus brightness, additional 979, 958, 937 and 916 pixels were plotted for one, two, three and four element frames (respectively). Each additional pixel was plotted to a corner of the display with {0, 0} x, y coordinates. This equalized the amount of pixels plotted in a single frame (although the extra pixels were invisible), thereby ensuring that: (i) stimulus frames were maintained at a constant 1 kHz presentation frequency; and (ii) each frame was equiluminant, despite changes in the amount of stimulus information presented.

Junction elements in the target display subtended at 1°17′ of the visual angle and were separated horizontally and vertically by between 2°42′ and 5°15′. Accordingly, target displays subtended 10°14′–13°03′ × 10°14′–13°03′ of the visual angle. Kanizsa figures represented a 'good square' with a probability of approximately 0.45 (see Shipley and Kelman, 1992). Each target junc-

tion consisted of 11 pixels and along each axis of the junction, the pixels were separated by 16′03″ of visual angle. The target display overall consisted of 99 pixels. According to an identical procedure to that used for premask displays, an additional 901 pixels were plotted to the corner of the display. This measure ensured that premask and target displays were equiluminant.

The EEG was recorded with NeuroScan amplifiers using 19 electrodes mounted in an elastic cap. Electrodes were placed according to the international 10–20 system. The ground electrode was C2 and all electrodes were referenced to the left mastoid (M1). Electrode impedance was kept below 5 kOhm. Horizontal and vertical EOG were registered with four additional electrodes. Data were sampled at 500 Hz and analog-filtered with a 0.05-Hz high-pass and a 100-Hz low-pass filter. Averaging epochs lasted from 200 ms before premask presentation to response-button press. All epochs were visually inspected for artifacts and rejected if eye movement artifacts or electrode drifts were visible. Baselines were computed in the −200–0-ms interval for each trial and subtracted prior to subsequent ERP analyses.

2.4. Analyses

Trials on which response errors were made (3.13% of all trials), were removed from the data, before the removal of RTs above or below 2.5 S.D. from the means of all (correct) observations (1.8% of all trials). As mentioned above, RT trials were rejected on the basis of eye movement artifacts or electrode drifts revealed in the EEG (1.4% of all trials). These measures were taken to provide the basis for complementary analysis of the RT and EEG data. Accounting for these measures, all subsequent RT and EEG analyses were performed on the mean scores calculated from an average of 75 trials for each experimental condition, for each observer.

The corrected RT data (shown in Table 1) were examined by means of a repeated measures analysis of variance (ANOVA) with main terms of prime (prime, no prime) and target (present, absent). On the basis of previous research (Elliott and Müller, 1998; Elliott and Müller, 2000), the evidence for priming was expected to be indicated by a significant target × prime interaction, revealing enhancements for prime presentations on target but not target-absent trials.

Visual inspection of the mean EEG amplitudes revealed prominent premask and target N1s and a target P300. The peak amplitudes of the N1 and P300 components were obtained by picking the most negative (N1), or most positive (P300) amplitudes within appropriate time windows for each observer and for each experimental condition. By this method, the amplitudes of the premask N1 were taken as the lowest within the period 100–200 ms following premask stimulus onset, and, for the target N1, were taken as the lowest amplitudes within the period 700–900 ms from premask display onset. For the target P300, the highest amplitudes were taken from the period 800–1050 ms from premask display onset (recall that the premask display was presented for 600 ms and immediately replaced by the target display, see also Fig. 2). The latencies of each peak amplitude were also recorded for subsequent analyses. A series of (repeated measures) univariate F tests examined the possibility that the position of the reference electrode on the left mas-

Table 1
(a) Mean target-present and target-absent RTs in ms (and associated S.E. mean) and (b) mean% errors (and associated S.E. mean) as a function of prime[a]

	Target-present		$R-S$	Target-absent		$R-S$
	Prime	No prime		Prime	No prime	
(a)	451 (7)	481 (8)	30	504 (8)	506 (9)	2
(b)	2.2 (0.67)	4.01 (0.88)		3.24 (0.82)	3.06 (0.91)	

[a]*Note*: $R-S$ refers to the mean difference between prime and no-prime RTs.

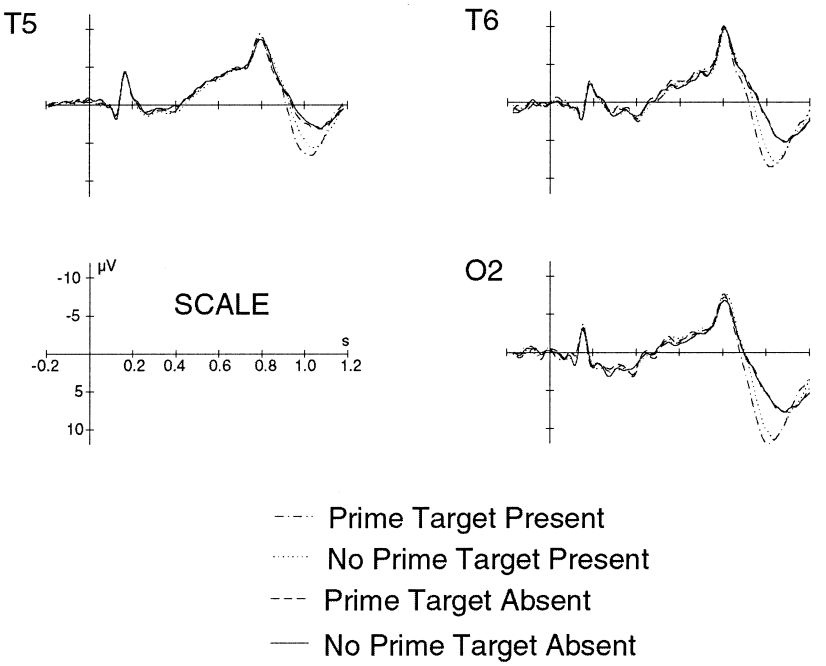

Fig. 2. Averaged ERPs for T5, T6 and O2 across an average trial duration of 1200 ms. ERPs are given for all combinations of target and prime conditions. The premask-display stimulus was presented across the first 600 ms of this period and was immediately followed by target-display presentation.

toid (M1) produced an asymmetry between the right and left hemisphere reference corrections of the EEG data. Tests were conducted for each ERP component (premask N1, target N1 and target P300) with a main term for hemisphere (right, left). For each test, hemisphere was revealed as non-significant ($F_{1,10} = 2.125$; $F_{1,10} = 0.776$; and $F_{1,10} = 2.816$, for the premask N1, target N1 and target P300, respectively), confirming that the referenced ERP amplitudes were not unilaterally biased by the position of the reference electrode.

The latency and amplitude of the N1 and P300 components at each electrode were collapsed across repeated measures and subject to principal components analyses (PCA), across observers and experimental conditions, to divide the ERP into a series of electrode subsets. The PCA is a standard, data-driven approach to analysis multiple time window and multiple electrode data with the purpose of identifying orthogonal, spatial sources of variance in the EEG (e.g. Donchin and Heffley, 1978; Donchin et al., 1997; Spencer et al., 1998; Spencer et al., in press). The PCA employed here used a correlational design with an equamax rotation, which aimed to classify the electrode amplitude/latencies into separate components (subsets) on the basis of maximum orthogonality between the mean amplitude/latencies and between the amplitude/latency subsets. The subsets of electrodes were defined for further analysis on the basis of eigenvalues > 1 and consisted of contributive amplitude/latencies (variables) with component weightings of ≥ 0.5. In practice, variable classification procedures terminated when weightings accounting for $> 50\%$ and $< 75\%$ of variance in each PCA had been extracted. Given that the target N1 potential was reliably obtained (for all observers) only at electrodes O1 and O2, no data reduction or classification procedures were applied to these data (note that the electrode subsets extracted from the PCAs conducted on the premask N1 and target P300 are given at the end of the following paragraph).

Examination of the EEG was conducted in three subsequent stages: firstly, a series of repeated-measures ANOVAs were conducted separately for all electrode subsets extracted from each PCA. These ANOVAs examined main terms for prime (prime, no prime), and electrode (variable, see below), with the additional factor target (present, absent) for the target N1 and target P300 responses. The principal object of the ERP analysis was to discover the loci of activity that displayed a similar pattern of effects to that revealed from analysis of the RT data. Specifically, and based upon the results of the RT data, the presence of target × prime and target × prime × electrode interactions in the target N1 and P300 components, with specific enhancements for primed relative to unprimed targets, were expected to indicate the likely loci at which activity across the prime and target interact. Analysis of the premask N1 was conducted with separate ANOVAs (excluding the factor target) for each of four subsets derived from the PCA. For the premask N1 the subsets consisted of: (i) amplitudes at frontal sites Fp1, Fp2, F4, F7 and F8; (ii) frontal and central amplitudes at Fz, F3, Cz, C3, C4 and T4; (iii) parietal amplitudes at Pz, P3 and P4; and (iv) occipito-parietal amplitudes at T5, T6, O1 and O2. Analysis of the target N1 was confined to occipital electrodes O1 and O2. For the target P300, amplitudes and latencies were also examined by means of separate ANOVAs for each of three subsets revealed by the PCA. These subsets could be characterized in terms of: (i) amplitudes distributed across frontal, central and temporal electrodes; (ii) centro-parietal amplitudes; and (iii) occipito-parieto-central latencies. Accordingly, the main terms for electrode in subsequent ANOVAs included: (i) amplitudes at T5, T3, T4, F3, F4, F7, F8 and FP1; (ii) amplitudes at P3, P4, CZ, C3, C4, FZ and FP2; and (iii) latencies at O1, O2, PZ, P3, P4, T5, T6 C3 and C4.

The second stage of analysis involved identical repeated measures ANOVAs to those performed on the ERP data. However, in this instance, the ANOVAs were performed on the 10-Hz and 40-Hz evoked EEG responses (time locked to premask display presentation) that co-occurred with the ERP and only for those electrode subsets within which target × prime interactions were revealed in the ERP data. For these time-frequency analyses, the ERP was convoluted with Morlet wavelets of the desired frequencies (10 and 40 Hz) to calculate specific frequency responses. The Morlet wavelet used here is calculated according to the following formula, which leads to sinusoidal waveforms.

$$\Psi(t) = e^{j\omega_0 t} e^{-t^2/2}$$

The wavelet was then compressed by a scaling factor α to obtain the desired frequency. By shifting the compressed wavelet with parameter b along the EEG signal, both the signal and the wavelet were convolved according to the following formula:

$$s_a(b) = \frac{1}{\sqrt{\alpha}} \int \overline{\Psi}\left(\frac{t-b}{\alpha}\right) x(t)\mathrm{d}t$$

where $\overline{\Psi}$ is the conjugate of the complex wavelet and $x(t)$ is the original EEG signal. To represent the phase-locked, time-frequency activity, wavelet transforms were computed across the average of single-trial data (WTAv, see below). Since the wavelet transform returns complex numbers, the absolute values were calculated. This time-frequency representation contains only that part of the activity that is phase locked to stimulus onset (i.e. the evoked gamma activity). For comparative purposes, note that in order to compute activity that is not phase locked to stimulus onset (and which cancels out in the grand average, i.e. the induced time-frequency activity), the sum of all activity should be calculated by averaging the absolute values of the wavelet transforms for the single-trial data (AvWT, see below). The application of this technique is detailed in full in Herrmann et al. (1999).

$$\mathrm{WTAv} = \left| \frac{1}{\sqrt{\alpha}} \int \overline{\Psi}\left(\frac{t-b}{\alpha}\right) \frac{1}{n} \sum_{i-1}^{n} x_i(t)\mathrm{d}t \right|$$

$$\mathrm{AvWT} = \frac{1}{n} \sum_{i=1}^{n} \left| \frac{1}{\sqrt{\alpha}} \int \overline{\Psi}\left(\frac{t-b}{\alpha}\right) x_i(t)\mathrm{d}t \right|$$

For the evoked time-frequency data, visual inspection of the amplitudes of the 10-Hz and 40-Hz responses to premask and target presentation found little variation across the range 8–12 Hz and 36–42 Hz (respectively).

The final stage of analysis involved the investigation of crosscorrelations between the (mean) subtraction of the prime from no-prime amplitudes, at 40-Hz, during the time period from premask-display onset to the target P300 response. These analyses were focused upon those electrodes at which a pattern of effects corresponding to the pattern of effects obtained in the RT data were obtained for the 40-Hz EEG response (i.e. those electrodes revealed as being of significance on the basis of a significant target × prime × electrode interaction).

3. Results

3.1. RT analysis

Analyses were conducted on the RT data prior and subsequent to correction for EEG artifacts and the pattern of effects was found to be identical. An ANOVA revealed no significant patterns within the error data. In addition, no speed-accuracy trade offs were revealed in the RT data.

Target-absent RTs were slower than target-present RTs [$F_{1,10} = 24.14$; $MS_e = 685.7$; $P = 0.001$; mean RT enhancement (and associated S.E. mean): 39 (8) ms]. Furthermore, the main effect of prime was significant ($F_{1,10} = 15.65$, $MS_e = 186.456$, $P < 0.005$). Consistent with previously reported findings (Elliott and Müller, 1998; Elliott and Müller, 2000), RT effects were confined to trials in which the flickering premask display was followed by a target Kanizsa figure [significant target × prime interaction: $F_{1,10} = 13.54$, $MS_e = 165.9$, $P < 0.005$; RT enhancements (and S.E. means) were 30 (8) ms and 2 (4) ms for target-present and target-absent conditions, respectively]. This result confirmed previously reported findings showing that figurally relevant information presented within premask-display flicker primes subsequent target detection.

3.2. EEG analyses

The ANOVAs conducted on the subsets of electrodes (revealed by the PCA analyses) for both premask and target N1's revealed no significant pattern of effects, although, as illustrated in Fig. 2, both the amplitude and latency of the target P300 was found to vary according to the presence or absence of a prime in the premask display. For the P300, the ANOVA performed on subset (i) (P300 amplitudes distributed across frontal, central and temporal electrodes) revealed no significant main effects or interactions in either the amplitudes of the ERP or 40-Hz responses. Even though the 10-Hz response varied across electrodes ($F_{7,70} = 5.563$, $MS_e = 0.0726$, $P < 0.001$) this was not significantly influenced by the presence of either target or prime. The ERP data from subset (ii) (P300 centro-parietal amplitudes) revealed a significant [2.5 microvolt (μV)] increase in (overall) amplitude for the target compared with the non-target response ($F_{1,10} = 11.5$, $MS_e = 45.532$, $P < 0.01$) and an increase in amplitude at central and posterior compared with frontal electrodes ($F_{6,60} = 7.67$, $MS_e = 41.12$, $P < 0.001$), although there was no main effect of prime nor any interactions with prime. As with subset (i), no pattern of effects were revealed from analyses of either the 10- or 40-Hz responses.

For subset (iii) (P300 occipito-parieto-central latencies) the ANOVA revealed a main effect for target ($F_{1,10} = 28.61$, $MS_e = 8688.6$, $P < 0.001$): target-present P300 latencies were faster than target absent latencies [mean latencies (and associated S.E. mean): 441 (12) and 491 (13) ms, respectively], while ERP latency on trials in which a prime was presented were, overall, faster than those in which no prime was presented (prime main effect: $F_{1,10} = 6.9$, $MS_e = 2607.83$, $P < 0.025$). Importantly, and consistent with the pattern of effects revealed in the RT data, the target × prime interaction was significant ($F_{1,10} = 10.21$, $MS_e = 3303.974$, $P = 0.001$) and was due to an earlier peak for prime compared with no-prime activity on target trials only [mean enhancements (and associated S.E. mean) 31 (12) ms and −5 (14) ms, for target-present and target-absent trials respectively; see Fig. 2]. No main effect was ob-

tained for electrode in subset (iii), nor were there any interactions with electrode, suggesting bilateral coherence in the P300 timing from central through posterior brain areas. Importantly, the target × prime interaction indicates an equivalent pattern of effects to those obtained from the RT data, which is supported by the similarity of the priming effects for the P300 and RT responses (i.e. 31 and 30 ms enhancements for target-present, compared with −5 and 2 ms for target-absent trials for the P300 and RT enhancements, respectively).

No specific loci were revealed from the ANOVA conducted on the amplitudes of the 10-Hz response (non-significant three-way interaction), although a significant target × prime interaction ($F_{1,10} = 6.05$, $MS_e = 0.0291$, $P < 0.05$) was based upon mean enhancements (no prime minus prime) of −0.56 μV for target-present and 0.28 μV for target-absent trials (respectively). A more specific indication of target priming was revealed in the corresponding evoked 40-Hz response, which accompanied the P300. For the 40-Hz response, neither target nor prime main effects were obtained, although the electrode main effect and a significant target × prime × electrode interaction were significant ($F_{8,80} = 4.55$, $MS_e = 0.0046$, $P < 0.001$; $F_{8,80} = 3.93$, $MS_e = 0.0011$, $P = 0.001$; note that the prime × electrode interaction was non-significant). The significant three-way interaction was explored by simple-main-effects analysis, which indicated the effects of prime presentation for target trials only at O2 [target present: $F_{1,10} = 81.92$, $P < 0.001$; target absent: $F_{1,10} = 0.027$, n.s, mean enhancements (and S.E. means) were 0.5 (0.02) and 0.07 (0.2) μV for target-present and -absent trials, respectively] and T6 [target present: $F_{1,10} = 8.94$, $P < 0.025$; target absent: $F_{1,10} = 0.038$, n.s, 0.4 (0.3) and 0.03 (0.5) μV for target-present and -absent trials, respectively; note that for the significant differences at O2 and T6, the no-prime response was significantly higher than the prime response]. Consistent with other findings (i.e. Hirsch et al., 1995), these results suggest that Kanizsa-type figures are coded in visuo-cortical mechanisms located principally in the right cortical hemisphere. The notion of a relationship between the figural priming effects obtained in the 40-Hz response amplitudes and the equivalent pattern of effects in the RT response gains additional support from the finding that the mean amplitude of the 40-Hz responses in O2 and T6 correlated well with the timing of RT response to the target Kanizsa-type squares. The partial correlations between the 40-Hz response amplitudes and the target-present RTs [which controlled for the 40-Hz activity at other electrodes in subset (iii)] were −0.651 and −0.029 ($P < 0.05$ and $P > 0.93$, for prime and no-prime conditions, respectively) at O2, and 0.902 and 0.911 ($P < 0.001$ and $P < 0.001$, for prime and no-prime conditions, respectively) at T6. Given the different patterns of partial correlation between the 40-Hz activity at O2 and T6 with the target-present RTs, activity at these electrodes was considered to relate differently to the process of RT response generation, with more evidence for figural priming in the differing correlations between RT and 40-Hz EEG for the prime and no-prime conditions at O2. Specifically and consistent with similar observations of 40-Hz activity during response execution reported elsewhere (e.g. Haig et al., 1999), the negative correlations obtained at O2 represent a reduction in 40-Hz amplitude accompanying target detection. One possible explanation for this finding is that the strength of 40-Hz target-coding activity over the right visual cortex is inversely proportional to the strength of 40-Hz activity induced during synchronous-premask presentation. In other words, a relatively strong pattern of existing and target-relevant 40-Hz activity appears to require a lower amplitude 40-Hz response during target detection, suggesting that some proportion of the 40-Hz response to target presentation has been prepared in advance by a synchronous-premask presentation. That the 40-Hz activity accompanying the P300 may be contrasted in terms of the priming of figure coding compared with the generation of a figurally-neutral spatio-temporal pattern of activity is supported by the absence of a correlation for no-prime conditions at O2. For the no-prime condition, an enhanced target response cannot logically result from the synchronization of neural assemblies specific to the spatial arrangement of feature elements across the target.

In summary, the pattern of results obtained from subset (iii) (P300 occipito-parieto-central latencies) are consistent with the idea that priming is a target-specific phenomenon, while in contrast to the ERP data, the corresponding evoked 40-Hz response offers more specific evidence for target priming and the associated RT effects at electrodes lying over primary visual and extrastriate visual cortex.

3.3. Cross-correlational analyses

Although the effects of target priming (i.e. the convergence of activity coding the target with that coding the prime) are evident in the 40-Hz EEG that accompanies the target P300 at O2 and T6, logically, the prime must have been generated at some point during premask-display presentation. As outlined in Section 1, it was suggested that a 40-Hz prime becomes active in the visual cortex, although prime generation is likely to require concurrent patterns of activity across more than one brain region, particularly in areas able to code across the spatial extent of the premask display. In addition, some distribution of prime activity across more than one cortical region would be necessary for coding and generating prime activity consistent with the 40-Hz frequency of premask-display frame presentation. This is logical, given that visuo-cortical neurons possess receptive fields of insufficient dimensions to code across the entire premask display, which rejects the possibility that the temporal structure of premask-display presentation is encoded exclusively by activity in early visual cortex (most likely to underlie electrodes positioned at O2 and T6). Instead, neurons within other visual processing regions (e.g. IT, MT of pre-frontal cortex) are able to respond to stimuli across a sufficiently wide region of visual space to account for the premask display as a whole and could, in principle, encode the temporal structure of premask display presentation.

In order to examine this hypothesis within the EEG, a cross-correlational analysis was employed following the standard formula described in most time series references (e.g. Box and Jenkins, 1976). Cross correlations were performed using the mean amplitude difference between the prime and no-prime conditions as this offered a more parsimonious account of the extent of priming at a given electrode and at a given point in time. The procedure used was as follows: for the 40-Hz response data for both prime and no-prime conditions, the mean amplitudes were calculated for each observer, at each electrode and across each of 11 consecutive 100-ms time windows (i.e. averaged across each successive presentation of the entire premask-display sequence from 0 to 600 ms, and in equivalent time steps, until the peak of the target P300 at between 1000 and 1100 ms). The mean amplitude differences were then calculated by subtracting the amplitude of the prime response from that of the no-prime response. In this way the extent of priming was correlated across different electrodes. Cross-correlational analyses were then performed between the 40-Hz prime responses at O2 and T6 with the 40-Hz subtractions at the remaining electrodes. Given that, overall, 36 cross correlations were calculated, a corresponding value of $\alpha = 0.0015$ was set for statistical significance. Significant cross-correlations are given in Table 2 and Fig. 3a; note that in each case the magnitude of the cross correlations exceeds the value of 0.7, described by Nunez et al. (1999) as the automatic correlation for volume conductance between electrodes separated by 4 cm or less. As illustrated in Fig. 3a, the pattern of cross correlations occurs exclusively about the lag of zero observations, which includes subtractions across temporal, parietal and central electrodes (T4, P3 and C3 for O2 and P4 for T6).

Inspection of both panels in Fig. 3b shows similar patterns of prime and no-prime 40-Hz

Table 2
Significant cross correlations (associated S.E. mean = 0.29) between priming effects at O2 and T6 with the 40-Hz subtractions at other electrodes[a]

O2	T6
T4 (0.802)	P4 (0.763)
P3 (0.802)	
C3 (0.781)	

[a] *Note*: All cross correlations are with lag 0 and differ significantly from chance performance with $\alpha \leq 0.0015$.

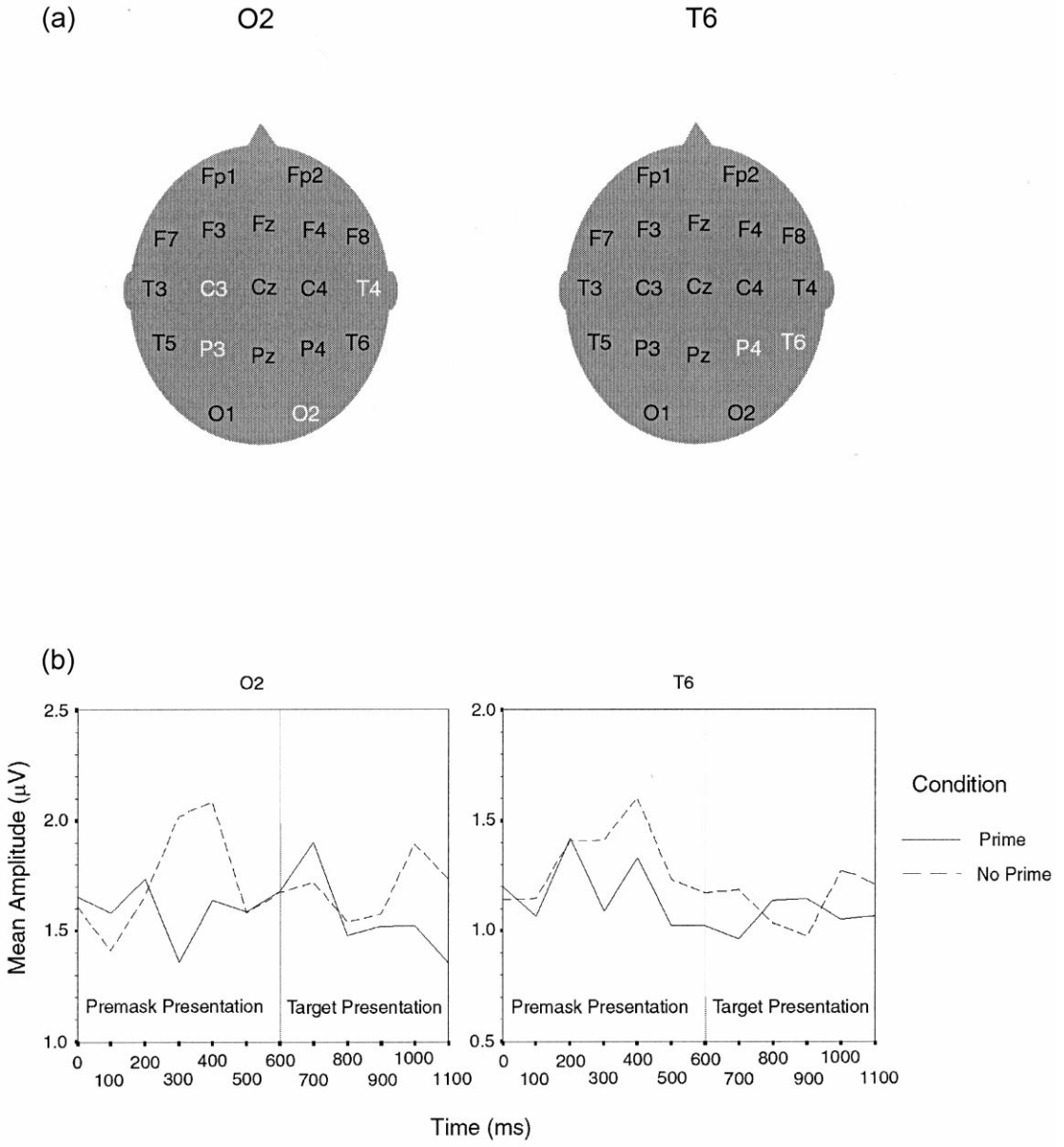

Fig. 3. (a) Significant cross correlations between the subtraction (the no-prime minus prime response) derived from the 40-Hz wavelet at O2 and T6 with the equivalent subtractions for the evoked 40-Hz response at other loci. Note that all cross correlations occurred with lag 0 and were computed for data collapsed across 11, 100 ms bins (i.e. across trial periods extending from trial onset at 0 ms to the P300 response at approx. 1100 ms). Given the number of comparisons (36), cross correlations were considered to differ significantly from chance (i.e. a correlation of 0.00) according to an α criterion of ≤ 0.0015. The cross correlations are also given in numeric form in Table 2. In (b), the mean amplitudes of the 40-Hz response for prime and no-prime conditions at O2 and T6 are plotted as a function of the time from premask display onset to the time period of the P300 (0–1100 ms). The reference line denotes the time of premask-display offset. Note the different slopes of the prime and no-prime conditions for O2 and T6 during the rise of the P300 (800–1100 ms).

activity. A major division between the 40-Hz prime and no-prime responses at both O2 and T6 occurs after 100 ms of premask-display presentation, which is characterized by an elevation of the no-prime response at between 200 and 300 ms, accompanied by a sharper decrease in the prime response at 200 ms. For both prime and no-prime responses, this pattern repeats at O2 during the rise of P300 activity to reach a maximum at 1100 ms. The positive cross correlations with activity at O2 (see Table 2) tend to indicate that the stimulus response at other electrodes exhibits a qualitatively similar character. This is supported by reference to Fig. 3b, which shows an elevated no-prime relative to a prime response at T6.

4. Discussion

Consistent with previously reported research, the RT data indicated that the presence of a figurally-relevant premask stimulus, embedded within a flickering premask display of distractor items, primes the subsequent presentation of a target according to the Gestalt configuration of the premask, even though the premask and subsequent prime are not detectable. Analysis of the parallel EEG data revealed that the statistical pattern obtained in the RT data was also found in the timing of the target P300 response at central, bilateral-parietal and occipital electrodes. The overall pattern of P300 timing across these loci did not, however, permit a more precise estimation of the locus for the RT priming effects, although a more precise correspondence between the RT and EEG priming effects was revealed within the evoked 40-Hz EEG over the right visual cortex (O2) and over extrastriate areas of the right ventral visual pathway (T6). Although this pattern of results is inconsistent with the idea that object representation may only occur as a property of induced gamma-band activity (i.e. Tallon-Baudry and Bertrand, 1999), this evidence supports other research revealing figurally-specific patterns of evoked gamma-band activity (Herrmann et al., 1999) and is entirely consistent with the idea that the prime becomes generated through the entrainment of figural coding mechanisms by a 40-Hz stimulus (see, Elliott and Müller, 1998; Elliott and Müller, 2000).

It was suggested in Section 1 that evidence of priming recorded temporal cortex (in this case at electrodes T3 and T4, which overlie the middle and superior temporal gyri; see Homan et al., 1987) might indicate the location at which the separate premask-display frames bring about a (combined) response at 40 Hz. Examination of Fig. 3a shows that the 40-Hz prime response at O2 does indeed correlate well with the 40-Hz subtraction at T4, which, like T6, lies over the right ventral visual pathway. As previously noted, given the non-detectability of the priming stimulus and spatial specificity of the priming effect (Elliott and Müller, 1998, Experiments 2 and 3), coupled with the finding that the prime exhibits a temporal structure and persistence consistent with the premask display as a whole, although the prime is most likely to be located in neural mechanisms underlying O2 and T6, the 40-Hz structure of the prime may be generated and subsequently back projected from neural mechanisms in IT, which underlies T4 in the right ventral visual pathway. This account is also consistent with the feedforward-feedback account of 40-Hz prime generation given by Elliott and Müller (2000).

The significant cross correlation of 40-Hz prime activity in both O2 and T6 with parietal electrodes (P3 and P4, respectively) cannot rule out the possibility that the spatial specificity of the priming effect is, to some extent, mediated by corresponding activity in the dorsal visual pathway, although the previous findings of Elliott and Müller (1998) argue against the priming effect as primarily dependent upon the deployment of spatial-attentional mechanisms (considered to be mediated by dorsal pathway mechanisms responding to transient signals in the visual field). Instead it seems possible that parietal mechanisms responding to the flicker across the premask display may also respond specifically to the Gestalt configuration within the flicker (as might be suggested by the findings of Logothesis and Schall, 1989). Allowing for facultative interactions between dorsal and ventral visual pathways, the contribution of parietal mechanisms may enhance, but are unlikely to be of singular signifi-

cance in generating figural priming in earlier stages. A similar conclusion may be assumed with regards to the cross correlation of activity in O2 with that in C3. C3 overlies the motor cortex and is likely to represent activity in the right hand (responsible for the target-present response). Accordingly, the possibility cannot be ruled out that generation of a 40-Hz code during visual coding also involves the generation of a response prime across mechanisms preparing the manual keypress. However, the RT data of Elliott and Müller (2000) examined the hypothesis that the 40-Hz prime was relatively non-specific to the Gestalt arrangement of synchronous-premask elements and found no evidence to support this notion, which tends to suggest the involvement of 40-Hz motor mechanisms support, rather than fully describe the 40-Hz priming effects.

One remaining puzzle concerns the differences between prime and no-prime activity at O2 and other related electrodes in which the no-prime activity achieves maximum amplitudes of a greater magnitude than those across the prime. This is shown in Fig. 3b, in which maximum 40-Hz amplitudes occur following 200–300 ms of premask-display presentation and later, with the rise of the target P300. One potential account for these phenomena includes the idea that, as the premask display is coded, the separate frames are represented in particular and different phases of the 40-Hz premask-display code. In no-prime conditions, the representation of elements across both the premask and subsequently the target displays would be coded within various phase angles determined by the location of those elements within the sequence of premask frames. During target coding, the convergence of target and premask activity early in visual processing might be expected to occur across neural assemblies coding local target elements. Accordingly, an additional latency (as was evident in the P300 response overall) combined with increased 40-Hz activity, might be expected if the neural mechanisms coding the target-display elements need to align the phase of their 40-Hz responses, which had been (randomly) shifted according to the asynchronous presentation of premask display elements at the locations subsequently occupied by the target Kanizsa-type square. The sharp increase in no-prime activity in O2 compared with the shallower slopes characterizing the no-prime responses in subsequent visual-coding areas such as T6 (see Fig. 3b) tends to support the idea that local visuo-cortical 40-Hz mechanisms are particularly susceptible to the effects of randomized premask-frame presentation. In contrast, for extrastriate neurons, receptive fields may be sufficiently large to code more than one (but not all) premask-display frames. Thus, some of the presentation asynchronies associated with premask-display frame presentation may become resolved by extrastriate neurons coding a sufficient degree of visual angle to account for the spatial separation between some of the premask frame elements. Consistent with the results shown in Fig. 3b, this should result in shallower 40-Hz target-coding activity due to the alignment of relatively fewer phase shifted neural assemblies during target coding. This account provides one hypothesis for examination in further RT and RT/EEG studies.

In conclusion, the influence of prime formation based upon the presentation of a flickering (40-Hz) visual-premask stimulus was revealed within the RTs to a subsequently presented target, with an equivalent pattern of effects obtained within the timing of the target P300 across central and posterior electrodes. A more specific pattern of effects was revealed from an analysis of the evoked 40-Hz response that accompanied the P300 at electrodes over visual cortex, specifically at O2 and T6. Subsequent cross-correlation analyses revealed that prime activity was distributed across occipital, parietal, temporal and central electrodes. On this basis, an account for Gestalt-prime generation was offered which emphasized the role of the right ventral visual pathway (responsible for visual Gestalt coding) for 40-Hz prime formation, which may be supported by both stimulus and task-specific activity recorded at parietal and central electrodes.

Importantly, the account of 40-Hz priming given here is based upon a parametric equivalence between the pattern of RT effects specific to visual-stimulus presentation within 40-Hz flicker, and a corresponding pattern of EEG effects re-

vealed within the evoked 40-Hz response to stimulus presentation. These findings not only support the role of a 40-Hz mechanism during figure-ground segmentation, but also suggest that patterns of oscillatory brain activity may be directly influenced by, and interpretable in terms of, equivalent patterns of stimulus activity.

Acknowledgements

This study is supported by Deutsche Forschungsgemeinschaft project grant No. SCHR 375/8-1. The authors' thanks are extended to D. Böttger and J. Wendt for assistance in subject recruitment and data analysis and to two anonymous reviewers for comments on an earlier draft of this manuscript. This work represents an equal contribution by the first two authors.

References

Başar, E., Başar-Eroglu, C., Demiralp, T., Schürmann, M., 1993. The compound P300-40 Hz response of the human brain. Elec. Clin. Neurophysiol. 87, 14.

Başar-Eroglu, C., Başar, E., 1991. A compound P300-40 Hz response of the cat hippocampus. Int. J. Neurosci. 13, 227–237.

Başar-Eroglu, C., Strüber, D., Kruse, P., Başar, E., Stadler, M., 1996a. Frontal gamma-band enhancement during multistable visual perception. Int. J. Psychophysiol. 24, 113–125.

Başar-Eroglu, C., Strüber, D., Schürmann, M., Stadler, M., Başar, E., 1996b. Gamma-band responses in the brain: a short review of psychophysiological correlates and functional significance. Int. J. Psychophysiol. 24, 101–112.

Bell, R.A., 1970. Application note 115. Principles of Cathode-Ray Tubes, Phosphors, and High-Speed Oscillography. Hewlett Packard Company/Colorado Springs Division, Garden of the Gods Road, Colorado Springs, Colorado, USA.

Box, G.E.P., Jenkins, G.M., 1976. Time Series Analysis: Forecasting and Control. Holden-Day, San Francisco.

Coltheart, M., 1980. Iconic memory and visible persistence. Percept. Psychophys. 27, 183–228.

Desimone, R., Albright, T.D., Gross, C.G., Bruce, C., 1984. Stimulus-selective properties of inferior temporal neurons in the macaque. J. Neurosci. 4, 2051–2062.

Donchin, E., Heffley, E., 1978. Multivariate analysis of event-related potentials: a tutorial review. In: Otto, D. (Ed.), Multidisciplinary Perspectives in Event-Related Potential Research (EPA-600/9-77-043). US Government Printing Office, Washington, DC, pp. 555–572.

Donchin, E., Spencer, K.M., Dien, J., 1997. The varieties of deviant expectancies: ERP manifestations of deviance processors. In: van Boxtel, G.J.M., Bocker, K.B.E. (Eds.), Brain and Behavior: Past, Present and Future. Tilburg UP, Tilburg, pp. 67–91.

Eckhorn, R., Frien, A., Bauer, R., Woelbern, T., Kehr, H., 1993. High frequency (60–90 Hz) oscillations in primary visual cortex of awake monkey. Neuroreport 4, 121–130.

Elliott, M.A., Müller, H.J., 1998. Synchronous information presented in 40-Hz flicker enhances visual feature binding. Psyc. Sci. 9, 277–283.

Elliott, M.A., Müller, H.J. (2000). Evidence for a 40-Hz oscillatory short-term visual memory revealed by human reaction time measurements. J. Exp. Psychol.: Learning Memory Cogn. 26(3), 703–718.

Engel, A.K., König, P., Kreiter, A.K., Singer, W., 1991. Interhemispheric synchronization of oscillatory neuronal responses in cat visual cortex. Science 252, 1177–1179.

Finley, G., 1985. A high-speed point plotter for vision research. Technical Note. Vis. Res. 25, 1993–1997.

Frien, A., Eckhorn, R., Bauer, R., Woelbern, T., Kehr, H., 1994. Stimulus-specific fast oscillations at zero phase between visual areas V1 and V2 of awake monkey. Neuroreport 5, 2273–2277.

Fujita, I., Tanaka, K., Ito, M., Cheng, K., 1992. Columns for visual features in monkey inferotemporal cortex. Nature 360, 343–346.

Gray, C.M., König, P., Engel, A.K., Singer, W., 1989. Oscillatory responses in cat visual cortex exhibit inter-columnar synchronization which reflects global stimulus properties. Nature 338, 334–337.

Gur, M., Snodderly, D.M., 1997. A dissociation between brain activity and perception: chromatically opponent cortical neurons signal chromatic flicker that is not perceived. Vis. Res. 37, 377–382.

Haig, A.R., De Pascalis, V., Gordon, E., 1999. Peak gamma latency correlated with reaction time in a conventional oddball paradigm. Clin. Neurophysiol. 110, 158–165.

He, S., Cavanagh, P., Intriligator, J., 1996. Attentional resolution and the locus of visual awareness. Nature 383, 334–337.

Herrmann, C.S., Mecklinger, A., Pfeifer, E., 1999. Gamma responses and ERPs in a visual classification task. Clin. Neurophysiol. 110, 636–642.

Hirsch, J., DeLaPaz, R.L., Relkin, N.R. et al., 1995. Illusory contours activate specific regions in human visual cortex: evidence from functional magnetic resonance imaging. Proc. Natl. Acad. Sci. USA. 92, 6469–6473.

Homan, R.W., Herman, J., Purdy, P., 1987. Cerebral location of international 10–20 system electrode placement. Elec. Clin. Neurophysiol. 66, 376–382.

Hubel, D.H., Wiesel, T.N., 1959. Receptive fields of single neurones in the cat's striate cortex. J. Physiol. London 148, 574–591.

Kreiter, A.K., Singer, W., 1992. Stimulus-dependent synchronization of neuronal responses in the visual cortex of the awake macaque monkey. J. Neurosci. 16, 2381–2396.

Livingstone, M.S., Hubel, D.H., 1988. Segregation of form, color, movement and depth: anatomy, physiology and perception. Science 240, 309–356.

Logothesis, N.K., Schall, J.D., 1989. Neuronal correlates of subjective visual perception. Science 245, 761–763.

Lutzenberger, W., Pulvermüller, F., Elbert, T., Birbaumer, N., 1995. Visual stimulation alters local 40-Hz responses in humans: an EEG study. Neurosci. Lett. 183, 1–4.

Moran, J., Desimone, R., 1985. Selective attention gates visual processing in the extrastriate cortex. Science 229, 782–784.

Müller, M.M., Bosch, J., Elbert, T. et al., 1996. Visually induced gamma-band responses in human electroencephalographic activity-a link to animal studies. Exp. Brain Res. 112, 96–102.

Müller, M.M., Junghöfer, M., Elbert, T., Rockstroh, B., 1997. Visually induced gamma-band responses to coherent and incoherent motion: a replication study. Neuroreport 8, 2575–2579.

Nunez, P.L., Srinivasan, R., Westdorp, A.F. et al., 1999. EEG coherency I: statistics, reference electrode, volume conductance, Laplacians, cortical imaging, and interpretation at multiple scales. Elec. Clin. Neurophysiol. 103, 499–515.

Shipley, T.F., Kelman, P.J., 1992. Strength of visual interpolation depends on the ratio of physically specified to total edge length. Percept. Psychophys. 52, 97–106.

Singer, W., 1996. Neuronal synchronization: a solution to the binding problem? In: Llinás, R., Churchland, P.S. (Eds.), The Mind–Brain Continuum: Sensory Processes. MIT Press, Cambridge, Mass, pp. 101–131.

Spencer, K.M., Mecklinger, A., Friederici, A.D., Donchin, E., 1998. Using a forest of electrodes to clear a garden path: Identifying the ERP components elicited by disambiguating words. Psychophysiology 35, S78.

Spencer, K.M, Dien, J., Donchin, E. (in press). A componential analysis of the ERP elicited by novel events using a dense electrode array. Psychophysiol.

Tallon, C., Bertrand, O., Bouchet, P., Pernier, J., 1995. Gamma-range activity evoked by coherent visual stimuli in humans. Eur. J. Neurosci. 7, 1285–1291.

Tallon-Baudry, C., Bertrand, O., 1999. Oscillatory gamma activity in humans and its role in object representation. Trends. Cogn. Sci. 3, 151–162.

Tallon-Baudry, C., Bertrand, O., Delpeuch, C., Pernier, J., 1996. Stimulus specificity of phase-locked and non-phase-locked 40 Hz visual responses in human. J. Neurosci. 16, 4240–4249.

Tallon-Baudry, C., Bertrand, O., Delpeuch, C., Pernier, J., 1997. Oscillatory γ-band (30–70 Hz) activity induced by a visual search task in humans. J. Neurosci. 17, 722–734.

Ungerleider, L.G., Mishkin, M., 1982. Two cortical visual systems. In: Ingle, D., Goodale, M., Mansfield, R. (Eds.), Analysis of Visual Behavior. MIT Press, Cambridge, MA, pp. 549–586.